

$|V_{cb}|$ AND $|V_{ub}|$ FROM CLEO

ANDREAS WARBURTON
(representing the CLEO Collaboration)

*Laboratory for Elementary-Particle Physics
Cornell University
Ithaca, New York 14853
USA*

*Department of Physics
McGill University
Montréal, Québec H3A 2T8
Canada*

I report on studies of inclusive and exclusive semileptonic $b \rightarrow cl\nu$ and $b \rightarrow ul\nu$ decays in 9.7 million $B\bar{B}$ events accumulated with the CLEO detector in symmetric e^+e^- collisions produced in the Cornell Electron Storage Ring (CESR). Various experimental techniques, including the study of spectral moments and the inference of neutrino candidates by exploiting the hermeticity of the CLEO detector, are used in conjunction with theoretical calculations to provide estimates of the CKM matrix elements $|V_{cb}|$ and $|V_{ub}|$.

*Invited talk presented at the 2003 QCD and Hadronic Interactions
session of the XXXVIIIth Rencontres de Moriond,
Les Arcs 1800, Savoie, France*

1 Introduction

High-precision measurements to help overconstrain the Cabibbo-Kobayashi-Maskawa¹ (CKM) quark-mixing matrix through its elements $|V_{cb}|$ and $|V_{ub}|$ are categorically blighted by the effects of long-distance QCD. Arguably, the impetus behind many recent theoretical advances in the non-perturbative QCD physics of meson decay has been to enable access to fundamental electroweak quantities like $|V_{cb}|$ and $|V_{ub}|$. The 4π solenoidal CLEO detector², which comprises tracking chambers, a CsI electromagnetic calorimeter, and muon systems, has enabled several new measurements^{3,4,5,6,7,8} of $|V_{cb}|$ and $|V_{ub}|$ through both inclusive and exclusive studies of moments and rates observed in semileptonic decays of B mesons produced in e^+e^- collisions at the Cornell Electron Storage Ring (CESR). Due to a dearth of space, we outline here briefly a new determination of $|V_{ub}|$ from extensive studies of exclusive $B \rightarrow [\pi, \rho, \omega, \eta]\ell\nu$ decays⁸, and refer the reader to recent publications^{3,4,5,6,7} for details of the other CLEO CKM measurements presented.

2 Event Reconstruction and Selection

Exclusive semileptonic decay studies are made difficult by the non-interacting neutrino, the kinematics of which can be inferred using the hermeticity of the CLEO detector by reconstructing missing energy ($E_{\text{miss}} \equiv 2E_{\text{beam}} - \sum E_i$) and missing momentum ($\vec{P}_{\text{miss}} \equiv -\sum \vec{p}_i$) in every event⁸. Within resolution, the signal neutrino combined with its companion charged lepton (ℓ) and meson (m) should satisfy constraints on energy, $\Delta E \equiv (E_\nu + E_\ell + E_m) - E_{\text{beam}} \approx 0$, and on momentum, $M_{m\ell\nu} \equiv [E_{\text{beam}}^2 - |\alpha\vec{p}_\nu + \vec{p}_\ell + \vec{p}_m|^2]^{\frac{1}{2}} \approx M_B$, where α is chosen to force $\Delta E = 0$. Events are examined with total charge $|\Delta Q| = 0$ or 1, and we reconstruct the momentum transfer $q^2 = M_{W^*}^2 = (p_\nu + p_\ell)^2$ from the missing momentum and the charged lepton's kinematics. Candidate charged leptons are required to have momenta $p_\ell > 1.0$ (1.5) GeV/ c for the pseudoscalar (vector) reconstructions.

3 Extraction of Branching Fractions

We performed a maximum likelihood fit⁸ in bins of the observables ΔE , $M_{m\ell\nu}$, ΔQ , 2π (3π) meson mass ranges in the $\rho\ell\nu$ ($\omega\ell\nu$) modes, and q^2 ; in total, the nominal fit involved 7 signal-mode topologies, comprised 259 bins, and had a χ^2 probability of 0.48. Projections of the nominal fit in the ΔE and $M_{m\ell\nu}$ variables in bins of q^2 and decay mode, as well as the various signal and background fit components, are indicated in Fig. 1. The experimental branching-fraction results are summarized in Tab. 1. By examining decay rates differentially in q^2 , we achieve a marked reduction in the sensitivity to theoretical model uncertainties originating from the form-factor shapes needed to simulate the signal and cross-feed fit components⁸. We emphasize that theoretical form factors do *not* constrain the relative rates across q^2 bins. For the $B^0 \rightarrow \pi^-\ell^+\nu$ ($B^0 \rightarrow \rho^-\ell^+\nu$) mode, we append to the total branching fractions listed in Tab. 1 residual theoretical form-factor uncertainties of $[\pm 0.01 \pm 0.07] \times 10^{-4}$ ($[\pm 0.41 \pm 0.01] \times 10^{-4}$) due to the signal and cross-feed components, respectively. To the $B^+ \rightarrow \eta\ell^+\nu$ total branching fraction, we append a model dependence¹¹ uncertainty of 0.09×10^{-4} .

4 Extraction of $|V_{ub}|$

We extract values of $|V_{ub}|$ using several approaches⁸ involving the measured rates for $\pi\ell\nu$ only, those for $\rho\ell\nu$ only, and an optimized combination of both mode types. Results from fits over the totality of phase space are indicated in Fig. 2, where the quality of fit can aid in discriminating between form-factor models by measuring how well the form-factor shapes describe the data. For example, in the $\pi\ell\nu$ case, the ISGWII¹¹ model receives only a χ^2 probability in the range 1 – 3% in our various fits, suggesting that this model is likely to provide less reliable $|V_{ub}|$ extractions.

As a preferred alternative, we employ a method to determine $|V_{ub}|$ that reduces modeling assumptions by exploiting theoretical QCD calculations solely in their q^2 regions of validity. In each of the $\pi\ell\nu$ and $\rho\ell\nu$ cases, we use form-factor shape and normalization results from light-cone sum rules

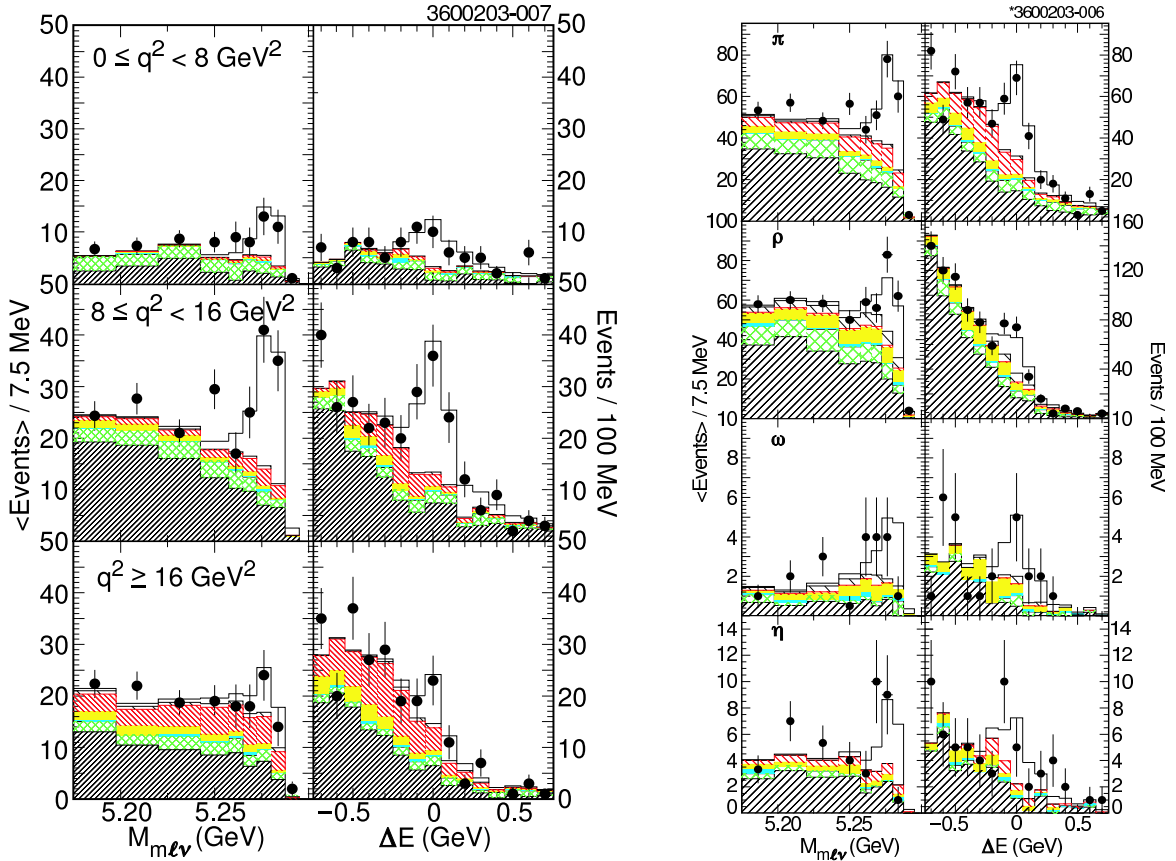


Figure 1: [left] $M_{ml\nu}$ and ΔE observables in the ΔE and $M_{ml\nu}$ signal band for the three q^2 bins (rows), requiring $\Delta Q = 0$ for the combined π^\pm, π^0 modes; [right] the same observables summed over the entire q^2 range for the combined π modes (top), ρ modes (row 2), ω (row 3), and η (bottom) modes. The points are the on-resonance data. The histogram components, from bottom to top, are $b \rightarrow c$ (fine 45° hatch); continuum (grey or green cross hatch); fake leptons (cyan or dark grey); feed down from other $B \rightarrow X_u \ell \nu$ modes (yellow or light grey); for the π^\pm and π^0 modes, cross feed from the vector and η modes into the π modes (red or black fine 135° hatch), cross feed among the π modes (coarse 135° hatch); for the ρ^\pm and ρ^0 modes, cross feed from the π and η modes into the ρ modes (red or black fine 135° hatch), cross feed among the vector modes (coarse 135° hatch); for the η mode, there is only a single cross-feed component from the non- η modes (red or black fine 135° hatch); and signal (open). The normalizations are those from the nominal fit.

Table 1: Summary of branching fractions from the nominal fit using the Ball'01⁹, Ball'98¹⁰, and ISGW II¹¹ form factors for the π , ρ , and η modes, respectively. The first uncertainties are statistical and the second systematic; the theoretical form-factor uncertainties are not listed⁸. The results for the fits with more restrictive charged-lepton momentum criteria in the vector modes are also shown. The q^2 intervals are specified in units of GeV^2 .

Mode	$\mathcal{B}_{q^2 \text{ interval}}$ $\times 10^4$	Vector-Mode Charged-Lepton Momentum		
		$p_\ell > 1.5 \text{ GeV}/c$	$p_\ell > 1.75 \text{ GeV}/c$	$p_\ell > 2.0 \text{ GeV}/c$
$B^0 \rightarrow \pi^- \ell^+ \nu$	$\mathcal{B}_{\text{total}}$	$1.33 \pm 0.18 \pm 0.11$	$1.31 \pm 0.18 \pm 0.11$	$1.32 \pm 0.18 \pm 0.12$
	$\mathcal{B}_{<8}$	$0.43 \pm 0.11 \pm 0.05$	$0.43 \pm 0.11 \pm 0.05$	$0.42 \pm 0.11 \pm 0.05$
	\mathcal{B}_{8-16}	$0.65 \pm 0.11 \pm 0.07$	$0.65 \pm 0.11 \pm 0.07$	$0.66 \pm 0.11 \pm 0.07$
	$\mathcal{B}_{>16}$	$0.25 \pm 0.09 \pm 0.04$	$0.24 \pm 0.09 \pm 0.04$	$0.24 \pm 0.09 \pm 0.05$
$B^0 \rightarrow \rho^- \ell^+ \nu$	$\mathcal{B}_{\text{total}}$	$2.17 \pm 0.34^{+0.47}_{-0.54}$	$2.34 \pm 0.34^{+0.43}_{-0.51}$	$2.29 \pm 0.35^{+0.40}_{-0.49}$
	$\mathcal{B}_{<8}$	$0.43 \pm 0.20^{+0.23}_{-0.23}$	$0.50 \pm 0.20^{+0.21}_{-0.22}$	$0.62 \pm 0.22^{+0.22}_{-0.23}$
	\mathcal{B}_{8-16}	$1.24 \pm 0.26^{+0.27}_{-0.33}$	$1.32 \pm 0.26^{+0.26}_{-0.29}$	$1.11 \pm 0.25^{+0.23}_{-0.25}$
	$\mathcal{B}_{>16}$	$0.50 \pm 0.10^{+0.08}_{-0.11}$	$0.52 \pm 0.10^{+0.08}_{-0.10}$	$0.56 \pm 0.10^{+0.07}_{-0.09}$
$B^+ \rightarrow \eta \ell^+ \nu$	$\mathcal{B}_{\text{total}}$	$0.84 \pm 0.31 \pm 0.16$	$0.84 \pm 0.31 \pm 0.16$	$0.83 \pm 0.31 \pm 0.15$

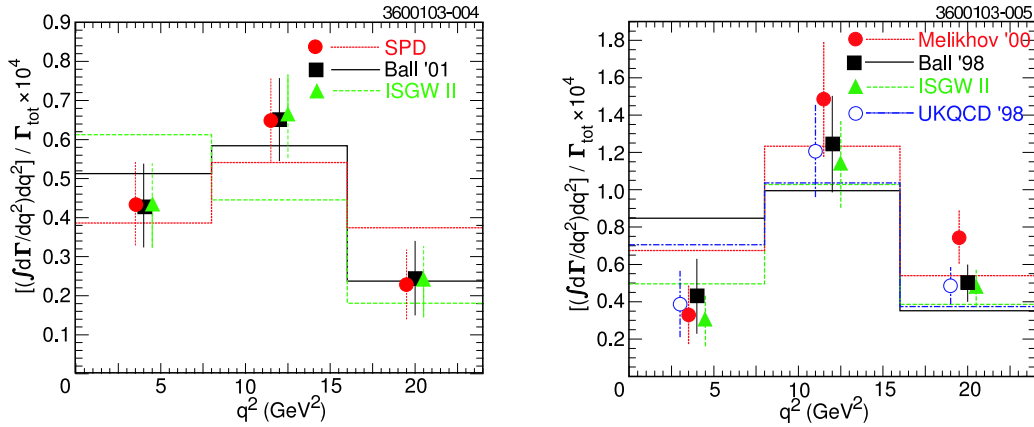


Figure 2: Measured branching fractions (points) in the restricted q^2 intervals for $B^0 \rightarrow \pi^- \ell^+ \nu$ [left] and $B^0 \rightarrow \rho^- \ell^+ \nu$ [right], and the best fit to the predicted $d\Gamma/dq^2$ (histograms) for various models (SPD – skewed parton distributions¹²; Melikhov'00 – a relativistic quark model¹³; UKQCD'98 – a lattice QCD calculation¹⁴) used to extract both rates and $|V_{ub}|$. The small horizontal offsets in the data points have been introduced for clarity.

(LCSR) QCD calculations⁸ in the region $q^2 < 16 \text{ GeV}^2$ and rate calculations from lattice QCD (LQCD) studies⁸ in the complementary $q^2 \geq 16 \text{ GeV}^2$ bin. In each of the $\pi\ell\nu$ and $\rho\ell\nu$ modes, we average the LCSR and LQCD results, taking into account correlated systematic uncertainties; we then combine the $|V_{ub}|$ results from the two mode types using an optimized weighting⁸. We find $|V_{ub}| = \left[3.17 \pm 0.17 \begin{smallmatrix} +0.16 \\ -0.17 \end{smallmatrix} \begin{smallmatrix} +0.53 \\ -0.39 \end{smallmatrix} \pm 0.03 \right] \times 10^{-3}$, where the uncertainties are statistical, experimental systematic, theoretical systematic based on the LCSR and LQCD uncertainties, and the $\rho\ell\nu$ form-factor shape uncertainty, respectively. Our results minimize our reliance on modeling and are consistent with previous rate and $|V_{ub}|$ measurements. Significant progress in the extraction of $|V_{ub}|$ from exclusive decays will require major theoretical improvements.

Acknowledgments

My colleagues in the CLEO collaboration and the CESR staff made these results possible. I am also grateful to McGill University for financial support.

References

1. N. Cabibbo, *Phys. Rev. Lett.* **10**, 531 (1963); M. Kobayashi and T. Maskawa, *Prog. Theor. Phys.* **49**, 652 (1973).
2. Y. Kubota *et al.* (CLEO), *Nucl. Instrum. Methods Phys. Res.* **A320**, 66 (1992); T. S. Hill, *Nucl. Instrum. Methods Phys. Res.* **A418**, 32 (1998).
3. S. Chen *et al.* (CLEO), *Phys. Rev. Lett.* **87**, 251807 (2001), [hep-ex/0108032].
4. D. Cronin-Hennessy *et al.* (CLEO), *Phys. Rev. Lett.* **87**, 251808 (2001), [hep-ex/0108033].
5. A. Bornheim *et al.* (CLEO), *Phys. Rev. Lett.* **88**, 231803 (2002), [hep-ex/0202019].
6. R. A. Briere *et al.* (CLEO), *Phys. Rev. Lett.* **89**, 081803 (2002), [hep-ex/0203032]; N. E. Adam *et al.* (CLEO), *Phys. Rev. D* **67**, 032001 (2003), [hep-ex/0210040].
7. A. H. Mahmood *et al.* (CLEO), *Phys. Rev. D* **67**, 072001 (2003), [hep-ex/0212051].
8. S. B. Athar *et al.* (CLEO), [hep-ex/0304019], and references therein, to appear in *Phys. Rev. D*.
9. P. Ball and R. Zwicky, *JHEP* **0110**, 019 (2001), [hep-ph/0110115].
10. P. Ball and V. M. Braun, *Phys. Rev. D* **58**, 094016 (1998), [hep-ph/9805422].
11. D. Scora and N. Isgur, *Phys. Rev. D* **52**, 2783 (1995), [hep-ph/9503486].
12. T. Feldmann and P. Kroll, *Eur. Phys. J. C* **12**, 99 (2000), [hep-ph/9905343].
13. D. Melikhov and B. Stech, *Phys. Rev. D* **62**, 014006 (2000), [hep-ph/0001113].
14. L. Del Debbio *et al.* (UKQCD), *Phys. Lett. B* **416**, 392 (1998), [hep-lat/9708008].